NeuroImage **11,** 13–23 (2000)
doi:10.1006/nimg.1999.0520, available online at http://www.idealibrary.com on IDEAL®

Cocaine Activation Discriminates Dopaminergic Projections by Temporal Response: An fMRI Study in Rat[1]

John J. A. Marota,* Joseph B. Mandeville,† Robert M. Weisskoff,† Michael A. Moskowitz,‡ Bruce R. Rosen,† and Barry E. Kosofsky§

**Department of Anesthesia and Critical Care, †Department of Radiology, ‡Department of Neurosurgery, and §Department of Neurology, Massachusetts General Hospital, Boston, Massachusetts 02114; NMR Center, MGH-East, Charlestown, Massachusetts 02119; and Harvard Medical School, Boston, Massachusetts 02115*

Received May 19, 1999

We applied a sensitive new functional magnetic resonance imaging technique to identify the pattern and determinants of cocaine-induced brain activation in drug-naive rats. At doses greater than 0.1 mg/kg iv, cocaine produced robust activation throughout cortex with the largest magnitude increase in frontal neocortex. Additionally, we detected selective activation within dopamine-innervated subcortical regions including dorsomedial and ventrolateral striatum, nucleus accumbens region, and dorsal thalamus. Although dose response was similar among activated regions, temporal response differentiated regions along distinct anatomical boundaries with basal ganglia and limbic cortical structures, reaching maximum activation later than frontal neocortex. Pharmacological specificity was demonstrated by blocking cocaine-induced activation with SCH-23390, a selective D1 antagonist. Our data demonstrate the utility of fMRI to identify spatiotemporal patterns of cocaine-induced brain activation and implicate D1 dopaminergic mechanisms in acute cocaine action.

INTRODUCTION

The effects of cocaine on the central nervous system are complex. Acute administration of cocaine in humans produces profound short-term euphoria while repeated drug exposure may result in drug addiction accompanied by dysphoria, anhedonia, and craving (Gawin, 1991). As the molecular, neurochemical, and neuroanatomic substrates for these complex behaviors are starting to be understood (Self and Nestler, 1995), several lines of evidence suggest that cocaine-induced stimulation of dopaminergic neurotransmission within cortical and subcortical limbic structures plays a pivotal role both in acute drug action and in initiating neural adaptations which contribute to drug dependence (Koob and Le Moal, 1997; Koob and Nestler, 1997; Koob and Bloom, 1988; Wise, 1996; Wise and Rompre, 1989). Therefore, elucidating anatomic and temporal patterns of regional brain activation following cocaine administration in naive and drug-dependent subjects may provide insights into the cascade of events bridging the acute and the chronic effects of cocaine.

Animal models of drug action and addiction are useful tools to characterize neurobiologic determinants of mechanisms underlying cocaine action (Hyman, 1996; Self *et al.,* 1996). Such models permit application of invasive technology that cannot be used easily to study humans, facilitate pharmacological manipulation of specific neurotransmitter systems and receptor subtypes, and enable comparison of drug effects in naive and chronically exposed or addicted animals. Functional magnetic resonance imaging (fMRI) provides a means to link mechanistic studies of drug action and addiction in animal models to recent studies of human brain activation by psychostimulants (Breiter *et al.,* 1997; Gollub *et al.,* 1996; Stein *et al.,* 1998).

The recent availability of a new class of paramagnetic contrast agents with long blood half-lives makes fMRI an important new tool for the study of drug action. These agents, not yet available for human use, significantly enhance the sensitivity of fMRI relative to endogenous contrast (Mandeville *et al.,* 1996; Kennan *et al.,* 1998; van Bruggen *et al.,* 1998; Palmer *et al.,* 1999) and, thereby, improve effective spatiotemporal resolution. Although autoradiographic techniques such as metabolic mapping with 2-deoxyglucose (Sokoloff *et al.,* 1977) or CBF mapping with iodoantipyrene (Sokoloff, 1981) have a much higher spatial resolution, the destructive nature of the approach restricts use to animal studies and obviously limits temporal resolution to a single time point per animal or an average change in activity integrated over a long time period. Because dynamic magnetic resonance imaging is nonin-

This work was supported by DA-09467, DA-00384 (J.B.M.), and DA-00354 (B.E.K.).

1053-8119/00 $35.00

vasive, a single subject can be studied multiple times, permitting the investigation of the evolution of a subject's response to an experimental challenge. In contrast, while positron emission tomography (PET) is nondestructive, it has reduced spatial and temporal resolution, which is particularly limiting in small animal studies. Furthermore, the low sensitivity makes acute drug studies challenging.

In this study, we employed a drug-naive rat model to identify the anatomical and temporal pattern of brain activation induced by cocaine. Using contrast-agent-enhanced fMRI, we mapped the magnitude and regional extent of changes in relative cerebral blood volume (rCBV) in response to cocaine in order to investigate regional differences in temporal and dose responses. In addition, we identified the importance of the D1 receptor in mediating fMRI activation produced by acute cocaine infusion. We report here anatomically distinct regional differences in the time course of activation with segregation of projections from the ventral tegmental area into regions of early or late response.

METHODS

Animal Preparation

All procedures were approved by the MGH Subcommittee for Research Animal Care in accordance with NIH guidelines. Male Harlan Sprague–Dawley rats (225–300 g) were anesthetized briefly with 1.5% halothane in oxygen for insertion of left femoral arterial and venous cannulae and placement of tracheostomy for mechanical ventilation (16-gauge intravenous catheter; Inste-W; Becton–Dickinson, Sandy, UT). All wounds were infiltrated with 1% lidocaine before incision. Following surgery, the inspired halothane concentration was reduced to 0.7% and rats were paralyzed with 2 mg/kg intravenous pancuronium, followed by a continuous intravenous infusion of 2 mg/kg/h. Pancuronium was dissolved in normal saline administered at 5 ml/kg/h. Rats were mechanically ventilated (small animal volume controlled ventilator; Harvard Apparatus, Inc., South Natick, MA) with an 80/20 air/oxygen mixture, an inspiratory to expiratory ratio of 1:1, and an initial tidal volume of 3.0 ml at a rate of 40 breaths per minute. Ventilation parameters were adjusted to maintain normal arterial blood gases (pH 7.40 ± 0.01, $P\mathrm{aCO_2}$ 40 ± 2, $P\mathrm{aO_2}$ 145 ± 10). One-hundred fifty-microliter blood samples withdrawn from the arterial cannula were analyzed for partial pressures of oxygen and carbon dioxide and pH (Ciba–Corning Model 1304) before administration of any drugs and at the conclusion of each experiment to ensure animal stability. Arterial blood pressure (ABP) and rectal temperature were monitored throughout experiments; rats were excluded from analysis if the mean ABP was less than 105 mm Hg. In a subset of animals, the arterial blood pressure waveform was collected, stored, and analyzed using MacLab/8 data acquisition and analysis system (ADInstruments, Mountain View, CA); heart rate was calculated from arterial pressure pulses by the data acquisition software. Rat torsos were wrapped in two heating blankets (Gaymar, Orchid Park, NY) circulating warm water to maintain core temperature at 37–38°C. To minimize MRI motion artifact, rats were placed into a custom plastic cradle attached to a head frame machined from delrin plastic (David Kopf Instruments, Fremont, CA); heads were fixed with plastic screws inserted into the ear canals and a bar inserted under the front incisors. Rat heads were shaved and covered with gel toothpaste to reduce magnetic susceptibility artifacts arising from air–tissue interfaces; ear canals and oropharynx were also filled with toothpaste. An MRI surface coil was secured over the dorsal surface of the head before positioning the animal in the magnet center.

Cocaine (RBI, Natick, MA) and SCH-23390 (RBI, Natick, MA) were dissolved in normal saline. Both drugs were administered as 0.5 ml bolus infusions at a rate of 1 ml/min via the femoral vein. Sixty minutes passed before repeat injections of cocaine.

Magnetic Resonance Imaging

Imaging studies were performed at a field strength of 2 T (SISCO spectrometer; Varian Spectroscopic Instruments, Palo Alto, CA). A 30-mm transmit and receive linear radio frequency surface coil was used in all studies for brain water excitation and detection. Prior to functional imaging, a multislice set of high-resolution conventional T_2-weighted coronal rat brain images was used to localize the anterior commissure. fMRI studies employed multislice gradient echo planar imaging of 9–15 contiguous coronal brain slices of 1 mm thickness with the first slice approximately 2 mm rostral to the anterior commissure; resolution in the image plane was 0.6 $\mathrm{mm^2}$. Images were acquired with gradient echo times of 25 ms and repetition times of 5 s; two averages were acquired for each time point for a temporal resolution of 10 s.

To significantly enhance fMRI sensitivity, a monocrystalline iron oxide nanocolloid (MION) with a very long blood half-life was injected at an iron dose of 12 mg/kg. MION was synthesized using previously described techniques (Shen *et al.,* 1993; Mandeville *et al.,* 1997); the biodistribution (Schaffer *et al.,* 1993) and physicochemical properties (Shen *et al.,* 1993; Jung *et al.,* 1996) have been reported. The blood half-life of MION is approximately 4 h in rats (Jung *et al.,* 1996); brain transverse relaxation rate following injection of unlabeled MION shows no detectable change for 3 h after equilibration in the blood (Mandeville *et al.,* 1997).

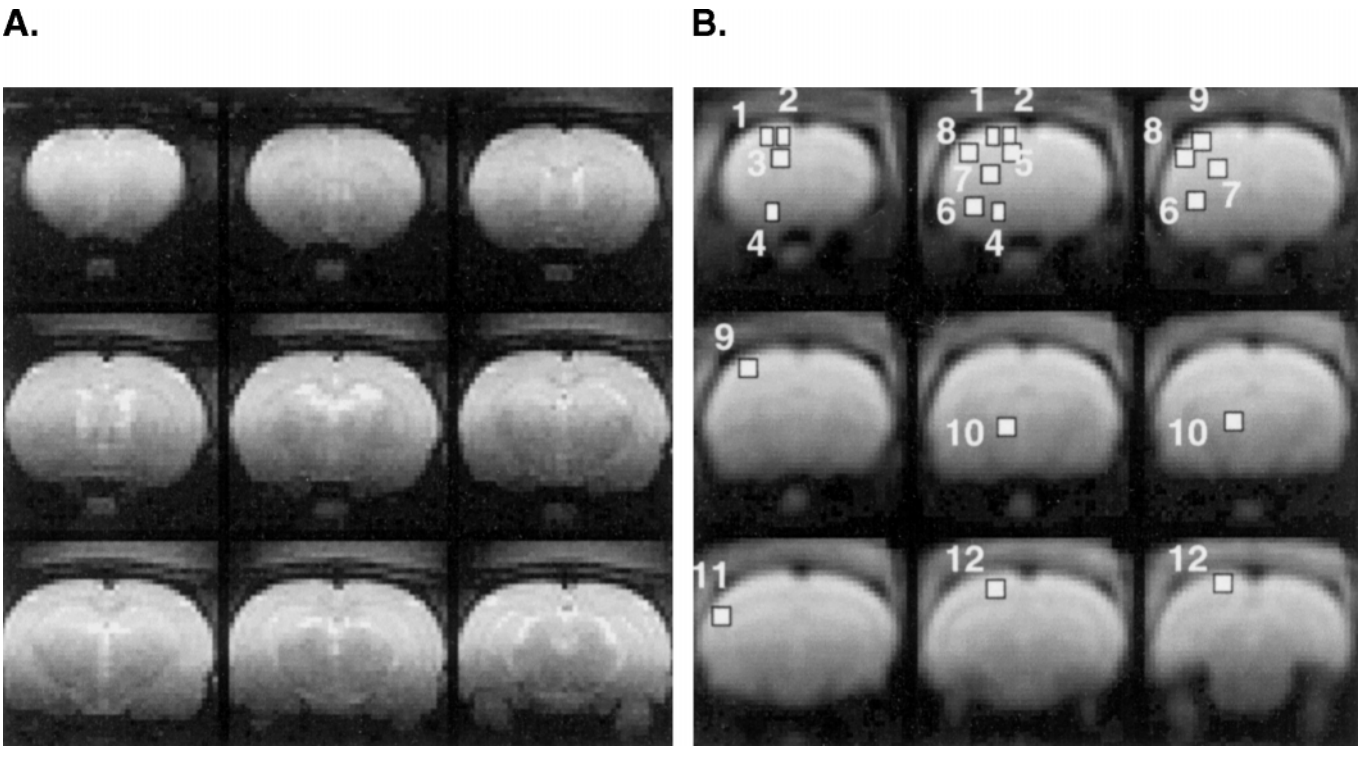

FIG. 1. (A) High-resolution conventional T_2-weighted images of the 1-mm brain slices used for analysis. (B) Echo planar images of the same slices as in A. The numbered overlays depict regions of interest for time- and dose-dependent analysis of rCBV: 1, AGl, agranular lateral frontal cortex; 2, AGm, agranular medial frontal cortex; 3, MPFC, medial prefrontal cortex; 4, N Ac, nucleus accumbens region; 5, A Cing, anterior cingulate cortex; 6, VL St, ventrolateral striatum; 7, DM ST, dorsomedial striatum; 8, SS WH, whisker barrel somatosensory cortex; 9, SS FP, forepaw somatosensory cortex; 10, D Thal, dorsal thalamus; 11, Aud, auditory cortex; 12, Vis, visual cortex.

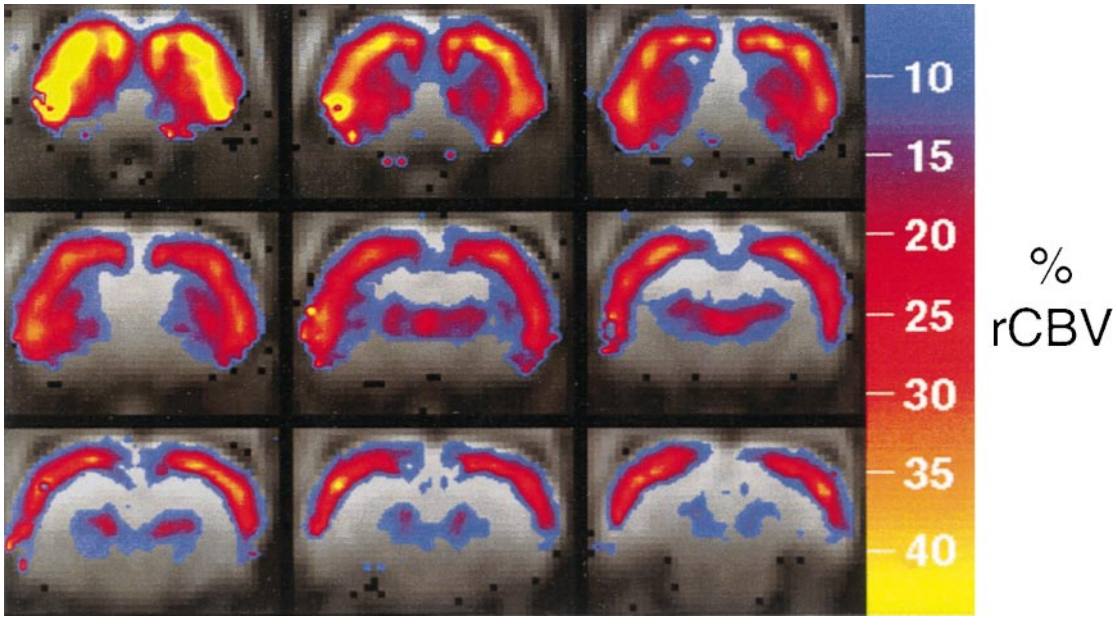

FIG. 2. Map of regional CBV response in rat after infusion of 1.0 mg/kg cocaine. Data are presented for nine consecutive 1-mm-thick coronal slices; the first slice is approximately 1 mm rostral to anterior commissure. The percentage increase in rCBV is depicted in pseudocolor (range 1–49%) overlying the gradient echo planar images.

Data Analysis

In order to generate average images of cocaine action, all functional image sets were manually registered onto the same brain template. The template was initially produced from a single data set. After registering many animals, the average brain image was used as the template; data that were registered to the initial template were then registered to the new template. To register data from an individual animal, first a multislice image set was generated by averaging images from many time points prior to cocaine infusion. This image set was then visually registered to the template using 6 degrees of freedom (3 shifts and 3 rotations). Since motion during data acquisition was not a problem due to anesthesia and paralysis, the 6 registration parameters determined for each rat were applied to all time points for that animal. Due to image distortions and anatomical variability, alignment error was estimated to be as large as 0.5 mm in each dimension, which reduced the effective image resolution to about 1 mm^3. Figure 1B shows the result of the registration procedure for one data set (nine animals); for anatomical reference, conventional spin-echo images acquired in a single animal are also shown (Fig. 1A).

After image registration, rCBV as a function of time (t) was calculated for each image voxel by assuming a linear relationship between the local blood volume fraction (V) and the change in transverse relaxation rate (ΔR_2^*) after injection of MION contrast agent, $\mathrm{rCBV}(t) = \Delta V(t)/V(0) = \Delta R_2^*(t)/\Delta R_2^*(0) - 1$, where ΔR_2^* was calculated from the echo time (T_E) and signals before (S_{PRE}) and after (S_{POST}) MION injection as $\Delta R_2^*(t) = -\ln(S_{POST}(t)/S_{PRE})/T_E$. Using this technique, hypercapnia-induced changes in CBV compared well with similar determinations made by PET and X-ray computed tomography (Mandeville *et al.,* 1998; Payen *et al.,* 1998; Zaharchuk *et al.,* 1998).

Brain maps of drug-induced changes in CBV were produced from the average temporal response to drug administration. For each time point, registered images from all animals in a group were averaged to produce a series of images which typically contained 30–60 images prior to drug administration and 150 images following drug injection. Each voxel was then subjected to a Student group t test between time points before injection and time points from 1 to 11 min after injection. To reduce false positives, a statistical threshold of $P < 0.01$ was subjected to a Bonferroni correction for the total number of brain voxels to reduce the threshold for significance to $P < 1 \times 10^{-7}$. For each voxel that reached statistical significance, percentage rCBV was indicated using a color scale overlaid on the average brain images. Separate maps were generated for positive and negative change in CBV.

A more conservative statistical test that did not take full advantage of the temporal information was applied to data in an analysis for regions of interest, which are defined in Fig. 1. For each animal, the average values of rCBV were calculated during the 5-min predrug baseline and from 1 to 11 min after drug infusion; the percentage change in rCBV was then calculated. These data were then subjected to a paired t test across the number of animals comparing pre- versus postdrug rCBV within each animal at each dose of cocaine.

An image-based analysis of the regional temporal response was performed. For each image voxel, the time to reach maximum response of rCBV following cocaine injection was calculated and indicated using a color scale overlaid on the average brain images. Prior to calculation of the time to peak, the temporal response of each voxel was subjected to a 5-min moving average to smooth signal fluctuations.

RESULTS

Acute intravenous cocaine infusion increased rCBV contrast signal in multiple regions of rat brain (Fig. 2). The map was generated by averaging results obtained from nine individual rats which received 1.0 mg/kg cocaine infusion. The color overlay indicates the percentage change in CBV for each voxel that reached a threshold of statistical significance of $P < 1 \times 10^{-7}$ assessed as a group t test comparison between pre- (baseline of 5 min before drug infusion) and postdrug infusion signal (from 1 to 11 min after cocaine). All nine rats studied showed a similar magnitude and regional pattern of activation. There was marked activation throughout the entire frontal cortex with extension into parietal and occipital regions. In all regions of cortex, the maximum increase in regional blood volume occurred within middle cortical layers. Activation of subcortical structures was also evident, with discrete regional increases within ventrolateral and dorsomedial striatum, nucleus accumbens region, and dorsal thalamus. At no time after cocaine infusion were any significant changes in CBV detected in any discernable portion of cerebellum, hippocampus, hypothalamus, midbrain tegmentum, medulla, or pons ($P > 0.05$ compared to predrug baseline in all regions). Although CBV did not decrease in any region of brain parenchyma, focal areas within large venous structures, including the sagittal and straight sinus and the venous plexus, within the transverse fissure did show positive signal changes; we attribute these to alteration in blood oxygenation within draining veins. There was no significant difference in the regional extent of activation when baseline signal was compared to postdrug infusion periods of 1 to 5, 12 to 21, or 1 to 25 min after cocaine infusion. As such, we could not identify any additional areas of activation nor any region which exhibited activation only at a later time period.

Because cocaine stimulates dopaminergic neuronal

transmission within brain, we examined the magnitude and duration of changes in CBV after cocaine infusion in 12 brain regions (defined under Methods) including 8 forebrain sites with rich (e.g., frontal cortex) and sparse (e.g., occipital cortex) dopamine innervation as well as 4 subcortical structures. Figure 3 illustrates the dose dependence of the magnitude of response to cocaine detected in these 12 regions. Infusion of 0.1 mg/kg cocaine produced a small effect on rCBV; in contrast, rCBV increased significantly at 0.5 mg/kg ($P < 0.0005$ all regions except dorsomedial striatum, $P < 0.0007$, and nucleus accumbens region, $P < 0.0025$) in all regions but showed no significant additional increase in magnitude at 1.0 mg/kg. Furthermore, there was no significant difference in regional extent of activation between 0.5 and 1.0 mg/kg. At doses of 5 mg/kg and higher, the response was associated with profound hypotension and cardiac arrhythmia, which confound interpretation of results (data not shown).

We were able to distinguish two distinct patterns of temporal response to cocaine infusion in rat brain. Figure 4A illustrates the regional distribution of this difference in temporal response after 1.0 mg/kg cocaine. The color overlay represents the time in minutes for each voxel to reach peak activation determined as maximum change in rCBV. As shown, there is a gradient in time to reach maximum activation with lateral neocortex exhibiting the fastest rise to peak within 3–5 min and striatum, nucleus accumbens region, and medial cortical regions, including the medial prefrontal and anterior cingulate cortex, reaching peak activation at 7–11 min. The time course of response of rCBV after 1 mg/kg cocaine in four representative regions is shown in Fig. 4B. We detected only a monophasic temporal response in all brain regions which exhibited a significant change in rCBV. Although all brain regions reached maximum activation either earlier (whisker barrel somatosensory cortex and dorsal thalamus) or later (medial prefrontal cortex and dorsomedial striatum) than 5 min post-cocaine infusion, the duration of response for all activated regions was similar; rCBV returned to baseline within 30 min. Furthermore, the rCBV did not fall below the predrug baseline level in any region after cocaine. There was no difference in either the regional pattern of anatomical distribution by temporal response or the duration of rCBV response following 0.5 or 1.0 mg/kg cocaine. The changes in rCBV cannot be due to simple alteration in cerebral perfusion as a result of blood pressure fluctuation since cocaine infusion was associated with only a transient and small (5–10 mm Hg) increase in arterial blood pressure which had resolved before a change in CBV was detected (Fig. 4C).

Because blockade of the D1 dopaminergic receptors has been shown to antagonize the effects of cocaine on both behavior and cerebral metabolism (Steketee and

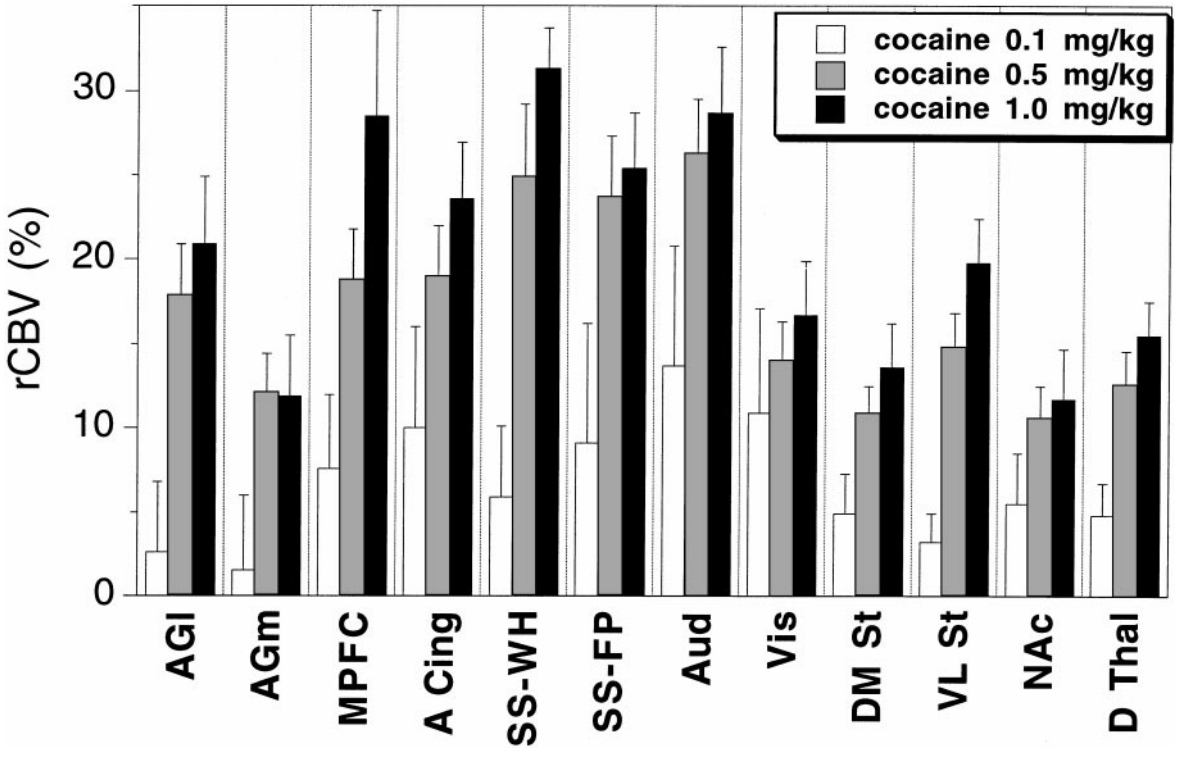

FIG. 3. Dose-dependent response after cocaine infusion in 12 brain regions. Data are presented as means ± SEM for percentage increase in rCBV for cocaine doses of 0.1 ($n = 6$), 0.5 ($n = 11$), and 1.0 mg/kg ($n = 9$).

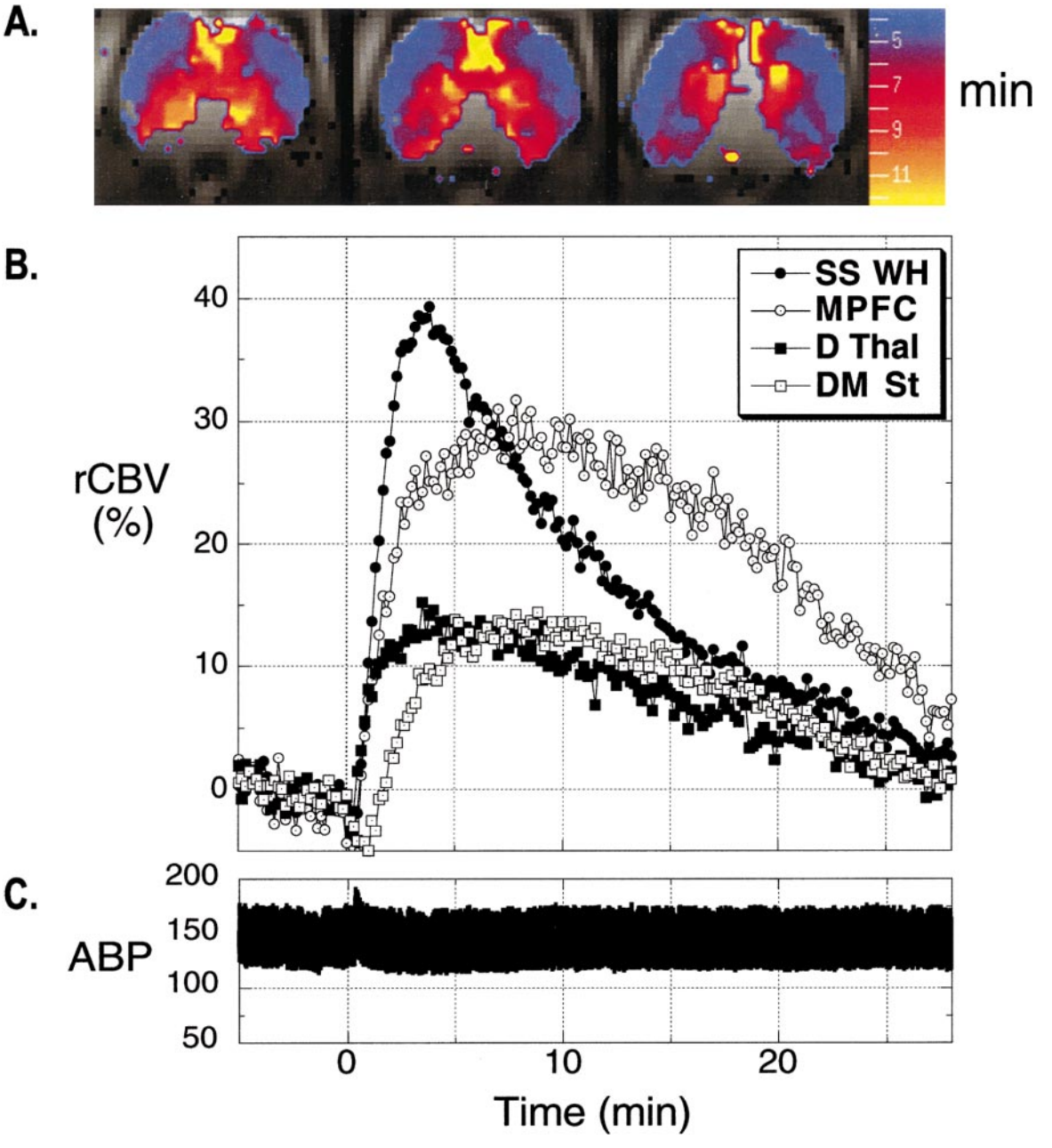

FIG. 4. (A) Map of time to reach maximum increase in rCBV after 1.0 mg/kg cocaine infusion. The pseudocolor overlay depicts the time in minutes for each voxel in which there was significant change in rCBV (same regions as in Fig. 1) to reach peak activation. Data are presented for three consecutive 1-mm-thick coronal slices; the first slice is approximately at the level of the anterior commissure (slices correspond to images 1, 2, and 3 in Fig. 1B). (B) Time-dependent changes in CBV within four brain regions of interest after 1.0 mg/kg cocaine infusion. Cocaine was infused at time 0 min. Data represent average percentage changes in CBV (n = 9) relative to a 5-min baseline obtained immediately before cocaine infusion.

Braswell, 1997; Baker *et al.,* 1998; Le *et al.,* 1997; Trugman and James, 1993), we examined the effect of SCH-23390, a selective D1 antagonist, on the fMRI pattern of cerebral activation induced by cocaine. Pretreatment of rats with 0.5 mg/kg SCH-23390 before infusion of 0.5 mg/kg cocaine blocked almost all cocaine-induced increase in rCBV (Fig. 5A) in all activated regions. Rats pretreated with 0.1 mg/kg SCH-23390 before infusion of 1.0 mg/kg cocaine (data not shown, n = 4) showed a similar blockade of cocaine-induced activation in all brain regions. Administration of SCH-23390 alone at either 0.1 or 0.5 mg/kg produced a small, region-specific decrease in rCBV in a distribution of structures similar to that in which CBV increased after

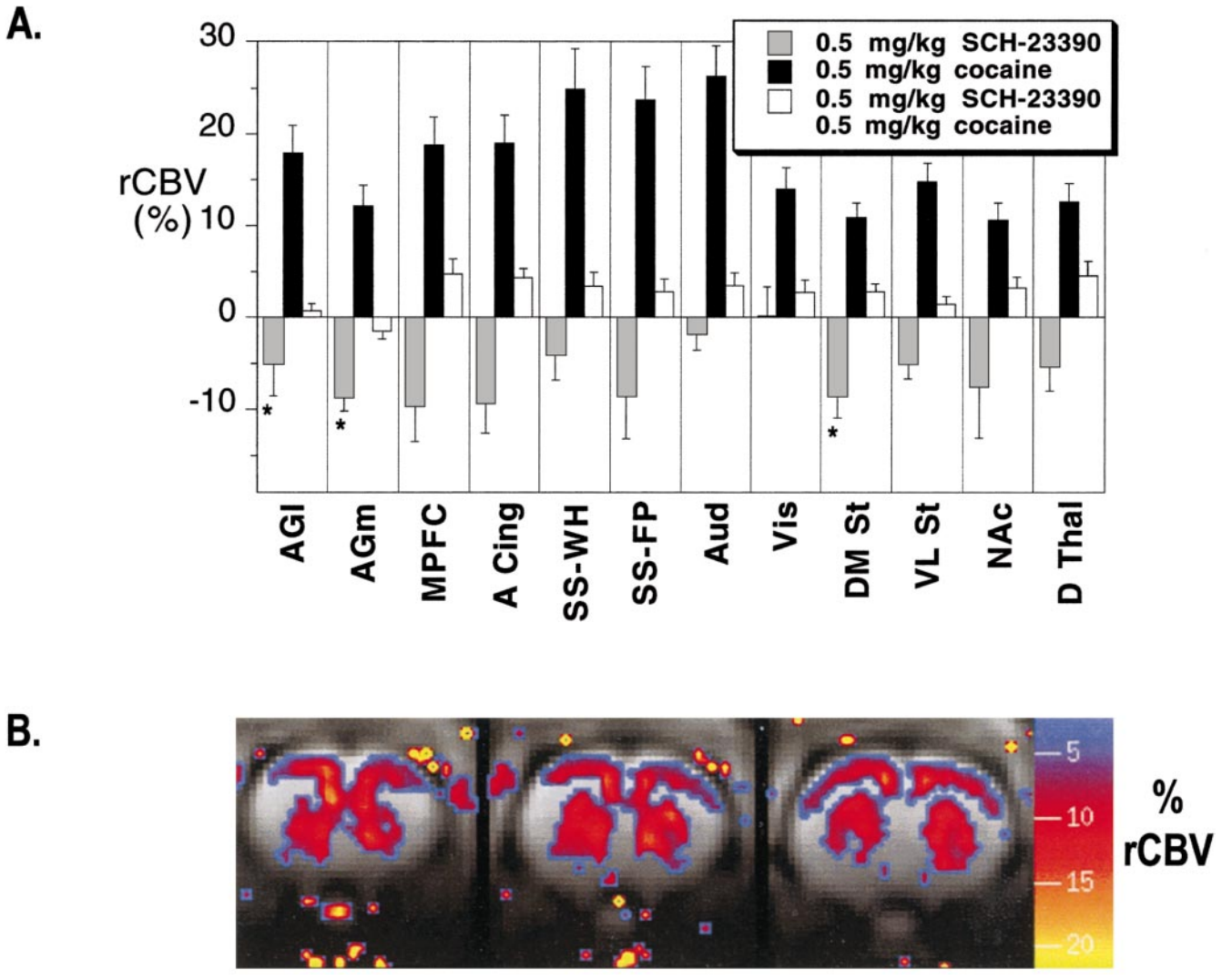

FIG. 5. (A) Magnitude of response in 12 brain regions after SCH-32290 ($n = 3$), cocaine ($n = 11$), and cocaine after pretreatment with SCH-23390 ($n = 3$). Data are presented as means ± SEM for percentage increase of rCBV. $^*P < 0.01$ by group t test comparison between average percentage changes in CBV relative to a 5-min baseline obtained immediately before drug infusion. For cocaine alone, all regions were significantly different from baseline; $P < 0.001$. (B) Map of decrease in regional CBV after infusion of 0.5 mg/kg SCH-23390. Data are presented for three consecutive 1-mm-thick coronal slices; the first slice is approximately at the level of the anterior commissure (slices correspond to images 1, 2, and 3 in Fig. 1B). The percentage decrease in rCBV is depicted in pseudocolor (range 2–23%) overlying gradient echo planar images.

infusion of cocaine without SCH-23390 pretreatment (Fig. 5B).

DISCUSSION

Functional MRI technology provides high spatial and temporal resolution for mapping region-specific brain activation. Since CBV-weighted fMRI significantly improves functional sensitivity relative to BOLD fMRI (Mandeville *et al.,* 1998), we chose this technique to map the regional activation pattern induced by acute cocaine infusion in the drug-naive rat. We observed a dose-dependent, region-specific activation of cortical and subcortical structures that was notably evident in regions with significant dopaminergic innervation. This activation can be suppressed by pretreatment with a D1 dopaminergic receptor antagonist before cocaine. Surprisingly, the temporal response of cocaine-induced activation discriminated regions within brain into late and early responding areas that were segregated along neuroanatomical boundaries.

Several lines of evidence argue strongly that the changes in fMRI signal described here are a direct consequence of cocaine-induced regional increases in brain activity and not due to simple systemic effects of cocaine or a global effect on cerebral vasculature. First,

we detected a pronounced region-specific pattern of activation after cocaine infusion with no increase in rCBV within the hippocampus, amygdala, or cerebellum and activation of only selected portions within the striatum and thalamus. Moreover, suppression of activation by a specific D1 dopaminergic receptor antagonist suggests a highly selective receptor-mediated process. Furthermore, identification of two distinct temporal responses of activation following bolus infusion indicates that simple plasma kinetics cannot account for the time course of brain activation. As such, it is difficult to reconcile cocaine-induced increases in rCBV as a global effect on vasculature. Finally, in contrast to the robust and prolonged response in CBV which lasted for over 20 min after cocaine infusion, we observed only small, transient alterations of blood pressure lasting less than 2 min (Fig. 4C). We conclude, therefore, that the pattern of brain activation we observed is a direct consequence of the selective action of cocaine on particular cortical and subcortical targets resulting in neural activation within specific structures.

The anatomic pattern of activation and dose response reported here agree closely with both previously reported region-specific increases in metabolic rate (Porrino, 1993; Porrino *et al.,* 1988; London *et al.,* 1986, 1990) and CBF (Stein and Fuller, 1992, 1993) following intravenous cocaine administration. Porrino reported significant increases in local cerebral glucose utilization in only the medial prefrontal and nucleus accumbens after 0.5 mg/kg cocaine, with significant increases in sensorimotor cortex, as well as ventral, dosomedial, and dorsolateral caudate and substantia nigra only after 1 mg/kg cocaine. Similarly, Stein *et al.,* reported significant increases in CBF in selective mesocortical and nigrostriatal structures after 0.75 and 1.0 mg/kg. We detected little difference in either magnitude or distribution of activated structures between 0.5 and 1.0 mg/kg. The larger extent of activation observed in our study at lower doses may reflect enhanced sensitivity of fMRI. It is of note, however, that the dose at which we first detect functional activation of brain by cocaine is similar to the dose at which rats begin to self-administer (Papasava *et al.,* 1981; Papasava and Singer, 1985). Finally, at intravenous doses of 5 mg/kg or more, we observed profound systemic effects similar to the results of Booze *et al.,* in awake animals (Booze *et al.,* 1997); such hemodynamic instability confounds interpretation of brain-mapping techniques.

One major difference between our experimental conditions and previously reported studies mapping cocaine-induced changes in brain activity is our use of general anesthesia in these experiments. Technical restrictions inherent to fMRI necessitate the use of anesthesia for rodent studies. As such, we chose light general anesthesia with halothane because previous studies have shown that both flow-metabolism coupling and responsiveness to stimulation are preserved (Hansen *et al.,* 1989; Lindauer *et al.,* 1993; Ueki *et al.,* 1992). Furthermore, preliminary results from parallel experiments conducted in our laboratory to identify cocaine-induced changes in regional metabolic activity mapped with 2-deoxyglucose methodology reveal good correlation in both regions and relative magnitudes of response between halothane-anesthetized and awake rats (Jones *et al.,* 1998).

By inhibiting reuptake of the catecholamines norepinephrine and dopamine and the indoleamine serotonin, cocaine is believed to exert its primary action in the central nervous system by potentiating activity of these neurotransmitters at nerve terminals (Gold *et al.,* 1985). The anatomic pattern of cocaine-induced activation described here, with predominantly frontal cortical activation and subcortical activation in striatum and nucleus accumbens region, strongly correlates with the spatial distribution of D1 receptor distribution (Mansour *et al.,* 1990; Fremeau *et al.,* 1991; Kosofsky *et al.,* 1995b) and dopaminergic innervation as reflected by tyrosine hydroxylase fiber density (Fallon and Moore, 1978; Bjorklund and Lindvall, 1984). The relevance of dopaminergic mechanisms is confirmed by our ability to block most, but not all, of the cocaine-induced signal by pretreating animals with the selective D1 antagonist SCH-23390. These data are consistent with the notion that some cocaine-induced "positive" activation mediated via the D1 receptor may occur in the setting of an additional nondopaminergic activation. Whether this reflects cocaine-induced noradrenaline- or serotonin-mediated neural activity is an area for future investigation.

It is interesting to note that SCH-23390 itself produced a small and sustained "negative activation" in an anatomic pattern of distribution similar to that of cocaine activation. This is consistent both with the distribution of D1 receptors in rat brain and with previous findings of region-specific decreases in metabolic rate after D1 blockade described by others (Trugman and James, 1993). Because rCBV decreased in these regions after SCH-23390, we conclude that there must be some element of resting dopaminergic metabolic activity mediated via the D1 receptor in these structures which is suppressed by blockade of the D1 receptor. Of note, however, the dorsomedial region of the striatum exhibited maximal negative activation induced by SCH-23390 (Fig. 5B), whereas cocaine-induced positive activation was greatest in dorsal–central striatum, an area which overlaps with maximal cocaine-induced c-fos activation (Young *et al.,* 1991; Steiner and Gerfen, 1993; Graybiel *et al.,* 1990; Kosofsky *et al.,* 1995a).

A key result of this study is the ability to discriminate between anatomical regions of activated brain by tem-

poral response. As shown in Fig. 2, structures responding to cocaine activation respect the general topography of ascending dopaminergic projections to the forebrain originating in the ventral tegmental area (VTA) and substantia nigra (Bjorklund and Lindvall, 1984; Fallon and Moore, 1978). Both the early and the late responding regions depicted in Fig. 4 are innervated by these ascending dopaminergic midbrain projections (Swanson, 1982). Early responding areas, however, localize predominantly to lateral neocortex and late responding regions represent medial allocortical areas including medial prefrontal cortex and anterior cingulate cortex. Although cocaine-induced activation discriminates these structures on a functional basis, cytoanatomical differences do exist between these two groups of projections. Specifically, the lateral neocortex has a relatively low density of dopaminergic projections with innervation restricted primarily to superficial cortical layers; the highest density of dopaminergic fibers is located in layer I. In distinction, medial allocortical areas have a high density of dopaminergic innervation with peak density at the layer I/II border in anterior cingulate cortex and at the layer IV/V border in MPFC (reviewed by Oades and Halliday, 1987). Additional factors which may contribute to these distinct temporal response profiles may include interconnectivity among limbic structures and the density and distribution of projections from other monoaminergic systems (e.g., serotonergic), as well as specific distribution of individual receptor subtypes. Although elucidation of the mechanism by which activation of a subset of VTA innervated structures is delayed relative to others will require additional studies, these data do indicate a selective differential effect of cocaine within dopaminergic innervated sets of brain regions.

It is worth comparing our results in drug-naive rats with parallel studies in humans with a cocaine-using history (Breiter *et al.,* 1997). While basic anatomical differences preclude direct comparison between rat and human cortical structures, there is notable overlap in that activated subcortical structures, including both striatum and nucleus accumbens, receive ascending dopaminergic input from the ventral tegmental area and substantia nigra. It is interesting to note that Breiter *et al.* also described a trend within subcortical regions, including the nucleus accumbens, to exhibit a prolonged response after acute cocaine exposure in human cocaine users. Despite rats being both drug naive and anesthetized, the similarity in activation patterns implies that some components of cocaine-induced brain activation are a direct consequence of dopaminergic mechanisms rather than cognitive state, past drug history, or behavioral correlates of drug-induced activation. Furthermore, since SCH-23390 can block most of the cocaine-induced brain activation, similar fMRI experiments in humans could suggest the extent to which dopaminergic mechanisms mediate aspects of cocaine-induced brain activation associated with euphoria.

In summary, this study reinforces the importance of ascending dopaminergic input to cortical and subcortical structures as a critical determinant of cocaine-induced brain activation at behaviorally relevant doses and implicates the importance of signal transduction via the D1 receptor. Furthermore, the identification of separate temporal responses within projections from the ventral tegmental area and substantia nigra suggests a new dimension of complexity to understanding the response of the central nervous system to activation by cocaine. Because of the significant overlap between our results and the regional and temporal activation pattern observed in humans, we are encouraged that further fMRI experiments in rodents to dissect the cellular and molecular basis for cocaine-induced brain activation will shed light on the neurochemical systems relevant in mediating cocaine-induced brain activation in human drug addicts with the ultimate goals of selective pharmacological intervention and treatment of cocaine addiction.

REFERENCES

Baker, D. A., Fuchs, R. A., Specio, S. E., Khroyan, T. V., and Neisewander, J. L. 1998. Effects of intraaccumbens administration of SCH-23390 on cocaine-induced locomotion and conditioned place preference. *Synapse* **30:**181–193.

Bjorklund, A., and Lindvall, O. 1984. Dopamine-containing systems in the CNS. In *Handbook of Chemical Neuroanatomy* (A. Bjorklund and T. Hokfelt, Eds.), pp. 55–122. Elsevier, Amsterdam.

Booze, R. M., Lehner, A. F., Wallace, D. R., Welch, M. A., and Mactutus, C. F. 1997. Dose–response cocaine pharmacokinetics and metabolite profile following intravenous administration and arterial sampling in unanesthetized, freely moving male rats. *Neurotoxicol. Teratol.* **19:**7–15.

Breiter, H. C., Gollub, R. L., Weisskoff, R. M., Kennedy, D. N., Makris, N., Berke, J. D., Goodman, J. M., Kantor, H. L., Gastfriend, D. R., Riorden, J. P., Mathew, R. T., Rosen, B. R., and Hyman, S. E. 1997. Acute effects of cocaine on human brain activity and emotion. *Neuron* **19:**591–611.

Fallon, J. H., and Moore, R. Y. 1978. Catecholamine innervation of the basal forebrain. IV. Topography of the dopamine projection to the basal forebrain and neostriatum. *J. Comp. Neurol.* **180:**545–580.

Fremeau, R. T. J., Duncan, G. E., Fornaretto, M. G., Dearry, A., Gingrich, J. A., Breese, G. R., and Caron, M. G. 1991. Localization of D1 dopamine receptor mRNA in brain supports a role in cognitive, affective, and neuroendocrine aspects of dopaminergic neurotransmission. *Proc. Natl. Acad. Sci. USA* **88:**3772–3776.

Gawin, F. H. 1991. Cocaine addiction: Psychology and neurophysiology. *Science* **251:**1580–1586.

Gold, M., Washton, A., and D., C. 1985. Cocaine abuse: Neurochemistry, phenomenology, and treatment. In *Cocaine Use in America: Epidemiologic and Clinical Perspectives* (N. J. Kozel and E. H. Adams, Eds.), pp. 130–150. U.S. Govt. Printing Office, Washington, DC.

Gollub, R. L., Breiter, H., Weisskoff, R., Kennedy, W., Kennedy, D., Kantor, H., Gastfriend, D., Berke, J., Riorden, J., Mathew, T.,

Makris, N., Guimaraes, A., Hyman, S., and Rosen, B. 1996. Cocaine induced global decrease in cerebral blood flow does not obscure regional activation detected by fMRI. *Soc. Neurosci. Abstr.* **22:**1933.

Graybiel, A. M., Moratalla, R., and Robertson, H. A. 1990. Amphetamine and cocaine induce drug specific activation of the c-fos gene in stiosome-matrix compartments and limbic subdivisions of the striatum. *Proc. Nat. Acad. Sci. USA* **87:**6912–6916.

Hansen, T. D., Warner, D. S., Todd, M. M., and Vust, L. J. 1989. The role of cerebral metabolism in determining the local cerebral blood flow effects of volatile anesthetics: Evidence for persistent flow-metabolism coupling. *J. Cereb. Blood Flow Metab.* **9:**323–328.

Hyman, S. E. 1996. Addiction to cocaine and amphetamine. *Neuron* **16:**901–904.

Jones, R. C. W., Chou, T., Marota, J.-J. A., Mandeville, J. B., Weisskoff, R. M., Moskowitz, M., Rosen, B., and Kosofsky, B. E. 1998. Dopaminergic influences on cocaine-induced regional brain activation: A 2DG study. *Soc. Neurosci. Abstr.* **24:**778.

Jung, C. W., Weissleder, R., Josephson, L., Bengele, H., and Brady, T. J. 1996. Physical properties of MION-46 and AMI-227. Int. Soc. Magn. Reson. Med., 4th Annual Meeting, p. 1681.

Kennan, R. P., Scanley, B. E., Innis, R. B., and Gore, J. C. 1998. Physiological basis for BOLD MR signal changes due to neuronal stimulation: Separation of blood volume and magnetic susceptibility effects. *Magn. Reson. Med.* **40:**840–846.

Koob, G. F., and Bloom, F. E. 1988. Cellular and molecular mechanisms of drug dependence. *Science* **242:**715–723.

Koob, G. F., and Le Moal, M. 1997. Drug abuse: Hedonic homeostatic dysregulation. *Science* **278:**52–58.

Koob, G. F., and Nestler, E. J. 1997. The neurobiology of drug addiction. *J. Neuropsychiatry Clin. Neurosci.* **9:**482–497.

Kosofsky, B. E., Genova, L. M., and Hyman, S. E. 1995a. Postnatal age defines specificity of immediate early gene induction by cocaine in developing rat brain. *J. Comp. Neurol.* **351:**27–40.

Kosofsky, B. E., Genova, L. M., and Hyman, S. E. 1995b. Substance P phenotype defines specificity of c-fos induction by cocaine in developing rat striatum. *J. Comp. Neurol.* **351:**41–50.

Le, A. D., Tomkins, D., Higgins, G., Quan, B., and Sellers, E. M. 1997. Effects of 5-HT3, D1 and D2 receptor antagonists on ethanol- and cocaine-induced locomotion. *Pharmacol. Biochem. Behav.* **57:**325–332.

Lindauer, U., Villringer, A., and Dirnagl, U. 1993. Characterization of CBF response to somatosensory stimulation: Model and influence of anesthetics. *Am. J. Physiol.* **264:**1223–1228.

London, E. D., Wilkerson, G., Goldberg, S. R., and Risner, M. E. 1986. Effects of L-cocaine on local cerebral glucose utilization in the rat. *Neurosci. Lett.* **68:**73–78.

London, E. D., Wilkerson, G., Ori, C., and Kimes, A. S. 1990. Central action of psychomotor stimulants on glucose utilization in extrapyramidal motor areas of the rat brain. *Brain Res.* **512:**155–158.

Mandeville, J. B., Marota, J. J. A., Keltner, J. R., Kosofsky, B. E., Burke, J., Hyman, S., LaPointe, L., Reese, T., Kwong, K., Rosen, B. R., Weissleder, R., and Weisskoff, R. M. 1996. CBV functional imaging in rat brain using iron oxide agent at steady state concentration. Int. Soc. Magn. Reson. Med., 4th Annual Meeting, p. 292.

Mandeville, J. B., Marota, J. J. A., Kosofsky, B. E., Keltner, J. R., Weissleder, R., Rosen, B. R., and Weisskoff, R. M. 1998. Dynamic functional imaging of relative cerebral blood volume during rat forepaw stimulation. *Magn. Reson. Med.* **39:**615–624.

Mandeville, J. B., Moore, J., Chesler, D. A., Garrido, L., Weissleder, R., and Weisskoff, R. M. 1997. Dynamic liver imaging with iron oxide agents: Effects of size and biodistribution on contrast. *Magn. Reson. Med.* **37:**885–890.

Mansour, A., Meador-Woodruff, J. H., Bunzow, J. R., Civelli, O., Akil, H., and Watson, S. J. 1990. Localization of dopamine D2 receptor mRNA and D1 and D2 receptor binding in the rat brain and pituitary: An in situ hybridization–receptor autoradiographic analysis. *J. Neurosci.* **10:**2587–2600.

Oades, R. D., and Halliday, G. M. 1987. Ventral tegmental (A10) system: Neurobiology. 1. Anatomy and connectivity. *Brain Res.* **434:**117–165.

Palmer, J. T., de Crespigny, A. J., Williams, S., Busch, E., and van Bruggen, N. 1999. High-resolution mapping of discrete representational areas in rat somatosensory cortex using blood volume-dependent functional MRI. *NeuroImage* **9:**383–392.

Papasava, M., Oei, T. P., and Singer, G. 1981. Low dose cocaine self-administration by naive rats: Effects of body weight and a fixed-time one minute food delivery schedule. *Pharmacol. Biochem. Behav.* **15:**485–488.

Papasava, M., and Singer, G. 1985. Self-administration of low-dose cocaine by rats at reduced and recovered body weight. *Psychopharmacology* (*Berlin*) **85:**419–425.

Payen, J.-F., Vath, A., Koenigsberg, B., Bourlier, V., and Decorps, M. 1998. Regional cerebral plasma volume response to carbon dioxide using magnetic resonance imaging. *Anesthesiology* **88:**984–992.

Porrino, L. J. 1993. Functional consequences of acute cocaine treatment depend on route of administration. *Psychopharmacology* (*Berlin*) **112:**343–351.

Porrino, L. J., Domer, F. R., Crane, A. M., and Sokoloff, L. 1988. Selective alterations in cerebral metabolism within the mesocorticolimbic dopaminergic system produced by acute cocaine administration in rats. *Neuropsychopharmacology* **1:**109–118.

Schaffer, B. K., Linker, C., Papisov, M., Tsai, E., Nossiff, N., Shibata, T., Bogdanov, A., Jr., Brady, T. J., and Weissleder, R. 1993. MION-ASF: Biokinetics of an MR receptor agent. *Magn. Reson. Imag.* **11:**411–417.

Self, D. W., Barnhart, W. J., Lehman, D. A., and Nestler, E. J. 1996. Opposite modulation of cocaine-seeking behavior by D1- and D2-like dopamine receptor agonists. *Science* **271:**1586–1589. [See comments].

Self, D. W., and Nestler, E. J. 1995. Molecular mechanisms of drug reinforcement and addiction. *Annu. Rev. Neurosci.* **18:**463–495.

Shen, T., Weissleder, R., Papisov, M., Bogdanov, A., Jr., and Brady, T. J. 1993. Monocrystalline iron oxide nanocompounds (MION): Physicochemical properties. *Magn. Reson. Med.* **29:**599–604.

Sokoloff, L. 1981. Relationships among local functional activity, energy metabolism, and blood flow in the central nervous system. *Fed. Proc.* **40:**2311–2316.

Sokoloff, L., Reivich, M., Kennedy, C., DesRosiers, M., Patlak, C., Pettigrew, K., Sakurada, O., and Shinohara, M. 1977. The [^{14}C]deoxyglucose method for the measurement of local cerebral glucose utilization: Theory, procedure, and normal values in the conscious and anesthetized albino rat. *J. Neurochem.* **28:**897–916.

Stein, E., and Fuller, S. 1993. Cocaine's time action profile on regional cerebral blood flow in the rat. *Brain Res.* **626:**117–126.

Stein, E. A., and Fuller, S. A. 1992. Selective effects of cocaine on regional cerebral blood flow in the rat. *J. Pharmacol. Exp. Ther.* **262:**327–334.

Stein, E. A., Pankiewicz, J., Harsch, H. H., Cho, J. K., Fuller, S. A., Hoffmann, R. G., Hawkins, M., Rao, S. M., Bandettini, P. A., and Bloom, A. S. 1998. Nicotine-induced limbic cortical activation in the human brain: A functional MRI study. *Am. J. Psychiatry* **155:**1009–1015.

Steiner, H., and Gerfen, C. R. 1993. Cocaine-induced c-fos messenger RNA is inversely related to dynorphin expression in striatum. *J. Neurosci.* **13:**5066–5081.

Steketee, J. D., and Braswell, B. C. 1997. Injection of SCH 23390, but not 7-hydroxy-DPAT, into the ventral tegmental area blocks the acute motor-stimulant response to cocaine. *Behav. Pharmacol.* **8:**58–64.

Swanson, L. W. 1982. The projections of the ventral tegmental area and adjacent regions: A combined fluorescent retrograde tracer and immunofluorescence study in the rat. *Brain Res. Bull.* **9:**321–353.

Trugman, J. M., and James, C. L. 1993. D1 dopamine agonist and antagonist effects on regional cerebral glucose utilization in rats with intact dopaminergic innervation. *Brain Res.* **607:**270–274.

Ueki, M., Mies, G., and Hossmann, K. 1992. Effect of alpha-chloralose, halothane, pentobarbital, and nitrous oxide anesthesia on metabolic coupling in somatosensory cortex of rat. *Acta Anaesthesiol. Scand.* **36:**318–322.

van Bruggen, N., Busch, E., Palmer, J. T., Williams, S. P., and de Crespigny, A. J. 1998. High-resolution functional magnetic resonance imaging of the rat brain: Mapping changes in cerebral blood volume using iron oxide contrast media. *J. Cereb. Blood Flow Metab.* **18:**1178–1183.

Wise, R. 1996. Neurobiology of addiction. *Curr. Opin. Neurobiol.* **6:**243–251.

Wise, R. A., and Rompre, P. P. 1989. Brain dopamine and reward. *Annu. Rev. Psychol.* **40:**191–225.

Young, S. T., Porrino, L. J., and Iadarola, M. J. 1991. Cocaine induces striatal c-fos-immunoreactive proteins via dopaminergic D1 receptors. *Proc. Natl. Acad. Sci. USA* **88:**1291–1295.

Zaharchuk, G., Bogdanov, A. A., Jr., Marota, J. J., Shimizu-Sasamata, M., Weisskoff, R. M., Kwong, K. K., Jenkins, B. G., Weissleder, R., and Rosen, B. R. 1998. Continuous assessment of perfusion by tagging including volume and water extraction (CAPTIVE): A steady-state contrast agent technique for measuring blood flow, relative blood volume fraction, and the water extraction fraction. *Magn. Reson. Med.* **40:**666–678.